# Modeling the Human P-glycoprotein Translocation Mechanism Using Targeted Molecular Dynamics

An Undergraduate Thesis Presented to
the Academic Faculty

by

**Ethan J. Speir**

In Partial Fulfillment of the Requirements for the Degree
B.S. Biology with Research Option
in the School of Biology

**GEORGIA INSTITUTE OF TECHNOLOGY**

**May 2012**

# MODELING THE HUMAN P-GLYCOPROTEIN TRANSLOCATION MECHANISM USING TARGETED MOLECULAR DYNAMICS

**Approved by:**

---

**Date: _____**

**Dr. Stephen Harvey, Co-Advisor**
School of Biology
*Georgia Institute of Technology*

---

**Date: _____**

**Dr. Nael McCarty, Co-Advisor**
Department of Pediatrics
*Emory University School of Medicine*

---

**Date: _____**

**Dr. Jung Choi, Professor**
School of Biology
*Georgia Institute of Technology*

# TABLE OF CONTENTS

## ACKNOWLEDGEMENTS

This work was undertaken in the laboratory of Dr. Stephen Harvey[1] in conjunction with the laboratory of Dr. Nael McCarty[2]. I would like to extend my utmost gratitude to both Dr. Harvey and Dr. McCarty, for it was only with their constant support and guidance that I was able to complete this study. Additionally, I would like to thank Shefaet Rahman[1], Jared Gossett[1], and Burak Boz[1] for their assistance with understanding the concepts and techniques of molecular modeling and dynamic simulations.

**[1] School of Biology, Georgia Institute of Technology**
310 Ferst Drive
Atlanta, Georgia 30332

**[2] Department of Pediatrics, Emory University School of Medicine**
2015 Uppergate Drive
Atlanta, GA 30322

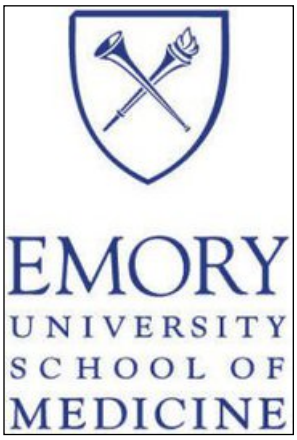


# ABSTRACT

**P-glycoprotein (P-gp), a member of the ABC-transporter superfamily, is a transmembrane protein that holds clinical importance due to its role in drug metabolism and multi-drug resistance (MDR) in cancer. Because crystallization attempts have failed at elucidating its 3D structure, recent research efforts have focused on constructing homology models of human P-gp. Prior to 2009, these homology models were primarily based upon bacterial transporters such as Sav1866, MalkK, and MsbA that represented the outward-facing conformation of P-gp. Following the release of an inward-facing mouse P-gp-based homology model of human P-gp, however, simulations modeling the inward- to outward-facing conformational change of P-gp have since been made possible. In this study, a targeted molecular dynamic (TMD) simulation is performed in order to model the translocation mechanism of human P-gp. This simulation provides insight into the gating scheme of P-gp itself as well as other ABC-transporters such as the cystic fibrosis transmembrane conductance regulator (CFTR), a protein implicated in the pathophysiology of cystic fibrosis.**

# 1. INTRODUCTION

## 1.1 P-glycoprotein

P-glycoprotein (P-gp), also known as multidrug resistance protein 1 (MDR1) or ATP-binding cassette sub-family B member 1 (ABCB1), is a transmembrane protein that in humans is encoded by the *ABCB1* gene [1]. Classified within ATP-binding cassette (ABC) superfamily, this protein is expressed in the apical membrane of many secretory cell types such as kidney, liver, intestine, adrenal gland, and the blood–brain barrier [2]. P-gp holds clinical importance due to its ability to bind to and export a wide variety of xenobiotic compounds, making it a significant factor for the absorption, distribution, metabolism and excretion of drugs [3]. This efflux mechanism of P-gp is particularly significant as it confers a multi-drug resistance (MDR) phenotype to cancer cells that have developed resistance to chemotherapy drugs [4]. For these reasons, P-gp has garnered strong research interest and has become the most extensively studied ABC-transporter.

P-gp consists of 1276-1280 amino acids with a molecular weight of approximately 170kDa. Like many other ABC-transporters, this protein contains transmembrane domains (TMDs) comprised of twelve highly hydrophobic α-helices (**Figure 1**). Located intracellularly are two nucleotide binding domains (NBDs) that act

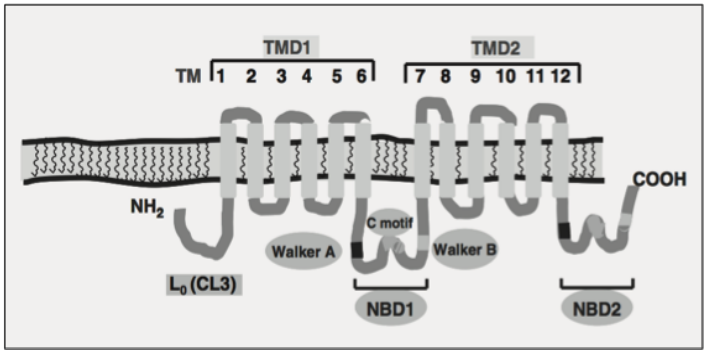


**Figure 1. Proposed topology of P-gp [5]**

as ATPase, hydrolyzing ATP and thereby generating the energy required for P-gp to actively pump substrate through the TMDs and across the membrane [5].

Due to the role that it plays in MDR of cancer cells as well as normal pharmacokinetics, P-gp has been identified as a key anti-target in modern drug discovery [6]. Preceding the ability to predict whether or not a lead compound will interact with P-gp, however, is an understanding of the mechanisms by which P-gp binds to and transports its many substrates. In accordance with the central dogma of molecular biology "Structure determines function", the first step in elucidating these mechanisms is to determine the 3D structure of this protein. Human P-gp, like many other membrane proteins, is difficult to crystallize. Even when expressed at high levels, P-gp does not purify well as surrounding lipid molecules interfere with crystallography and nuclear magnetic resonance (NMR) spectroscopy [7]. As a result, high-quality 3D structures of P-gp do not yet exist. Researchers, therefore, have recently begun to pursue an indirect method of structure prediction called homology modeling.

### 1.2. Homology modeling and existing P-gp models

Homology modeling is the process by which a 3D model, or homology model, for a protein of unknown structure is constructed based upon sequence similarity to proteins of known structure (**Figure 2**) [8]. The first step of homology modeling is to identify the template protein by aligning the primary amino acid sequence of the target protein to a large database of related sequences all with known 3D structures.

This process, known as multiple sequence alignment, scores each sequence entry in the database on its similarity to the target sequence. The entry with the highest degree of homology serves as the template protein. In regions of high correlation between the target and template primary - sequence, local structure of the target sequence can be deduced based on the known structure of the template sequence. In the second step, spatial constraints are applied to individual residues of the target sequence by quantifying these deductions. Finally, using modeling software, an atomic-resolution model of the target protein can be created using its primary amino acid sequence and the appropriate spatial constraints from the template protein.

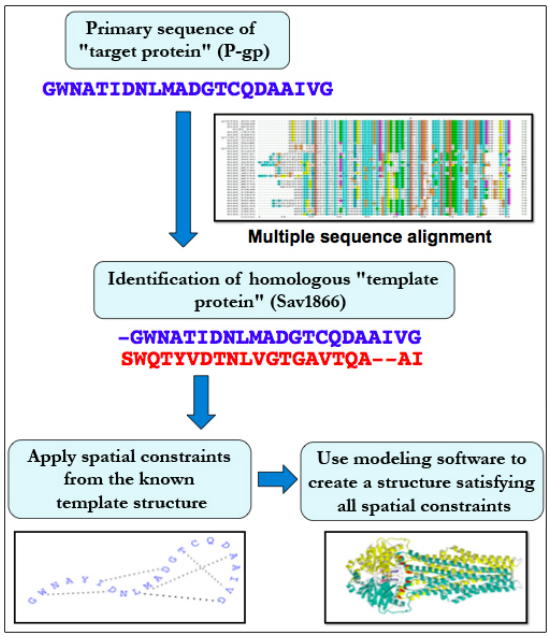

**Figure 2. Overview of homology modeling**

Development of human P-gp homology models has flourished recently following the emergence of several 3D structures of bacterial ABC-transporters such as Sav1866, MalK, and MsbA [9-12]. *Staphylococcus aureus* Sav1866-based homology models remain the most robust and complete structures of P-gp in the ATP-bound closed or "outward-facing" state. This is because i. all three MsbA crystal structures have been retracted due to data misinterpretation [13] and ii. MalK-based models require extrapolation of TMD structure as they only provide information on NBD conformation. Sequence identity between Sav1866 and P-gp differs markedly for each

domain, ranging between 12.9-15.8% in the TMDs to 44.6-48.4% in the NBDs. Sequence similarity between the two proteins, however, is much higher; 52.8-56% in the TMDs and 77.8-80.4% in the NBDs [10]. Such similarity in sequence confers a high degree of secondary structure conservation, making Sav1866 an ideal template for the outward-facing conformational state of human P-gp (outP-gp) as demonstrated in the model created by Callaghan et al (**Figure 3b**) [14].

Prior to 2009, homology models representing the inward-facing state of P-gp were limited by crude template proteins such as MsbA [12] or incomplete templates such as MalK [10]. In a seminal study by Aller et al, an X-ray structure of mouse P-gp with 87% sequence identity to human P-gp was produced, thereby providing a far-superior template for the inward-facing conformational state of human P-gp (inP-gp) [15]. Several models of inP-gp based on this structure have since been presented [16, 17], including that of Tarcsay et al in 2011 (**Figure 3a)** [18].

Considerable evidence exists suggesting that the P-gp translocation mechanism occurs through ATP-induced NBD dimerization, which results in conformational change between at least two distinguishable states. This has been inferred through experiments [19] and simulations on homologous ABC-transporters such as MalK [20]. Crystal structures of ABC-transporters in open [21], semi-open [22], and closed states [23] provide further support for this assumption. A recent study utilized FRET analysis to demonstrate that P-gp fluctuates between two major conformations during steady state turnover [24]. Despite all these findings, there is still very little

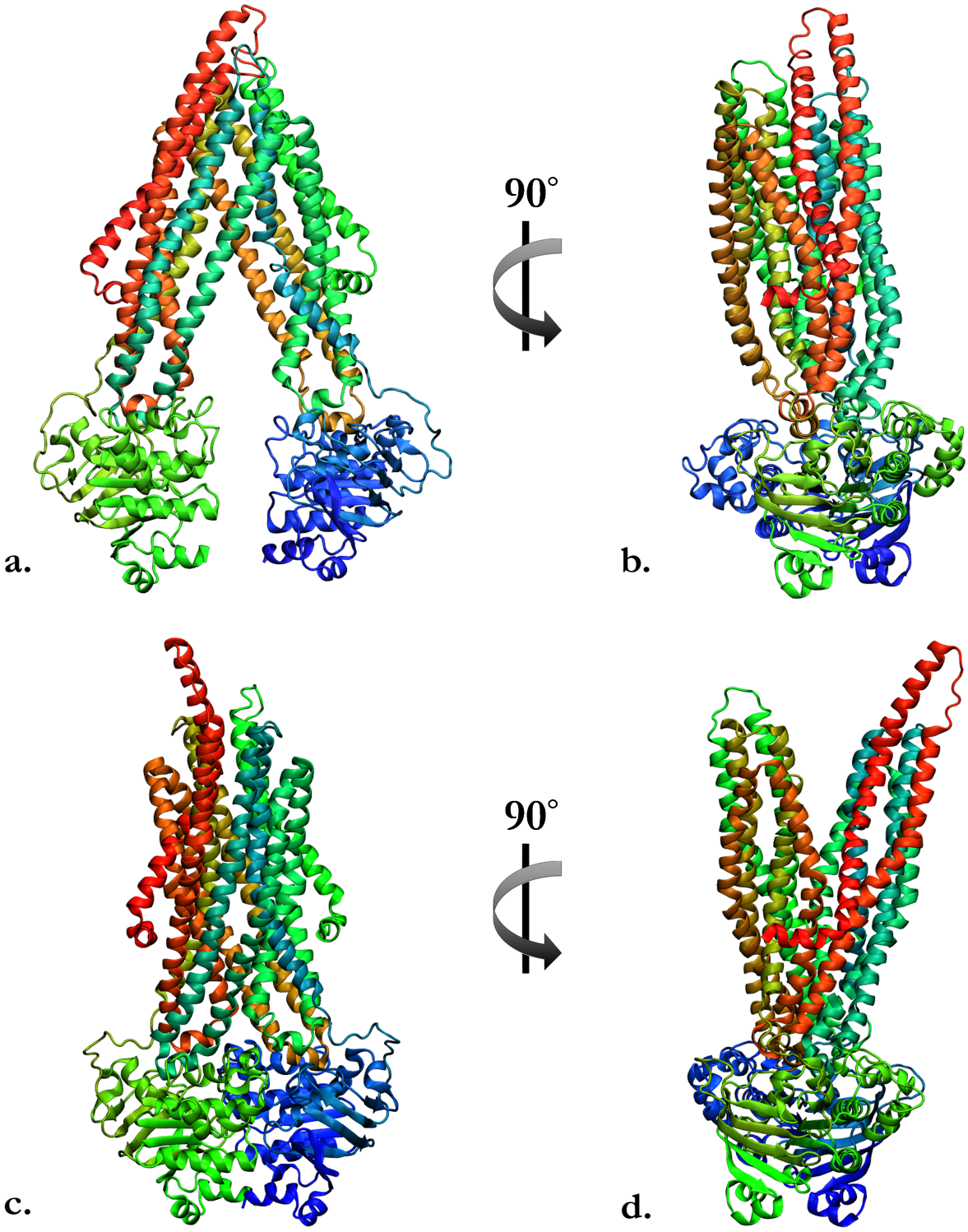


**Figure 3. Representations of (a and b) the mouse P-gp-based homology model [18] and (c and d) the Sav1866-based homology model [14] of human P-gp. These structures were used to define the inward- and outward-facing conformational states (respectively) for targeted molecular dynamic simulations.**

understanding of the precise mechanism that would result in multiple P-gp conformational states. One can immediately understand the value of a creating a molecular dynamics simulation modeling the translocation mechanism of P-glycoprotein as it exists in membrane.

Molecular dynamic simulations based upon structures deduced by homology modeling is a technique that has been used to model the conformational changes exhibited in a number of proteins including $H^+K^+$ ATPase proton pumps [25], G protein-coupled receptors (GPCRs) [26], and even ABC-transporters such as the bacterial vitamin B(12) transporter BtuCD [27]. To date however, no equivalent simulation has been reported for human P-gp despite the recent emergence of mouse P-gp-based inward-facing homology models that, in conjunction with existing outward-facing structures, would be make such a simulation possible. Therefore, the objective of this study is to design the first-ever targeted molecular dynamics simulation of the P-gp translocation mechanism using pre-defined homology models.

### 1.3. Molecular dynamics

Molecular dynamics simulations are computational-based processes by which a molecular model is animated at an atomic level over a brief timescale, such as pico- or nanoseconds, in order to represent the innate "jigglings and wigglings of atoms" [28]. Molecular dynamics simulations can be used to find a pathway between multiple conformational states of a protein such as P-gp. One specific method through which this is done is targeted molecular dynamics (TMD). In this approach, the protein is

guided from one conformation to another by means of an external steering forces, typically calculated as a function of the distance between the current and target positions of the atoms [29, 30].

It is important to note that, due to computational limitations, the timescale of the TMD simulation reported in this study are not equivalent to that of actual molecular processes. Despite this, however, several recent studies have shown that dynamic simulations can still produce qualitatively accurate pathways for actual conformational change [25-27, 31-33].

### 1.4. Relevance to CFTR and other ABC-transporters

P-gp, as mentioned before, is a member of the ATP-binding cassette (ABC) transporter superfamily. Due to their vital role in transport of a wide variety of substrates including drugs, metabolites, and lipids, ABC-transporters, when mutated, can result in several serious diseases.

Cystic fibrosis (CF) is a recessive genetic disorder regarded as the most lethal genetic disease among Caucasian populations. CF results from mutations in the cystic fibrosis transmembrane conductance regulator (*CFTR*) gene responsible for encoding the CFTR protein, a member of the ABC-transporter superfamily [34]. Although over 1,500 such mutations have been described, the structural consequences of these mutations are difficult to understand due to lack of success in crystallizing CFTR [35, 36]. Recent efforts have crystallized certain domains of CFTR, however the overall 3D structure still remains largely undefined [37]. This challenge has

stimulated a flourish of homology modeling studies beginning in 2008 when Riordan and colleagues created the first-ever CFTR homology model [38].

Currently, there exist three notable homology models for CFTR based upon the crystal structure of Sav1866 [39-41]. These models putatively represent the outward-facing or open conformation of CFTR and, as a result, do not allow for deduction of the gating scheme between open and closed conformational states. By creating a CFTR homology model based upon a protein representing the inward-facing or closed conformation such as mouse P-gp, molecular dynamics simulations can be performed in order to elucidate CFTR's gating scheme.

The simulation reported in this study can yield a realistic picture of the structural changes accompanying the gating cycle of both P-gp itself and that of ABC-transporters that use the mouse P-gp structure as a template for homology modeling. Given the structural similarities between P-gp and CFTR, such as the fact that they both have twelve transmembrane helices and highly conserved NBDs, some assumptions of the CFTR gating scheme can be made based upon what is observed during the P-gp simulation. For instance, if certain helices rotate or translate from a buried position towards a pore-facing conformation over the course of the simulation, these helices may play an important role in the CFTR gating scheme, as they are most likely important for defining the ion channel. Deductions such as this can facilitate the creation of a more robust simulation of the CFTR gating scheme.

Development of a simulation representing CFTR's gating scheme has profound pharmaceutical and clinical significance. As such a simulation would allow for determination of specific residues critical to ion conduction function, it would enable identification of potential drug binding sites required to lock CFTR into an open conformation. This would increase $Cl^-$ secretion, improve osmotic flow out of epithelial cells, reduce mucus aggregation, and potentially ameliorate the effects of cystic fibrosis.

## 2. MATERIALS

Visual Molecular Dynamics (VMD) version 1.8.7 was used for all molecular visualization and analysis purposes in this study [42]. Various plugins featured in this application were used to construct the membranous environment. This software was run on a 2.4 GHz dual-core MacBook using Mac OS X 10.7.3.

All molecular dynamics simulations were completed using NAMD version 2.7 [43]. Simulation runs utilized the high performance computing (HPC) facility overseen by the Georgia Tech Partnership for an Advanced Computing Environment (PACE). Although the quantity of processors and runtime varied for different simulation runs, final TMD production runs required full use of 48 processors for over 28 hours.

# 3. METHODS

A TMD simulation was performed to model the translocation mechanism of human P-gp, or the inward- to outward-facing (I→O) transition. Before this simulation could be completed, however, a membranous environment was first constructed in order to emulate the conditions of P-gp *in situ* (**Figure 4**).

## 3.1. Defining conformational states of P-gp

The first and most crucial step in simulating human P-gp was to identify the conformational states of the protein. After extensive literature review, the outward-facing state was chosen to be defined by the Sav1866-based homology model set forth by Callaghan et al in 2007 [14]. The mouse P-gp-based homology model published by Tarcsay et al in 2011 was chosen to represent the inward-facing state of human P-gp [18]. The pdb coordinates for these two models were graciously provided by the respective research groups upon request.

As the homology models, upon receipt, had different orientations in space, both were aligned to their respective template proteins as they exist in membrane. Information on the spatial arrangements of these template proteins was provided by the Orientations of Proteins in Membranes (OPM) database, which positions proteins in a lipid bilayer of adjustable thickness by minimizing the transfer energy of the protein from water to the membrane [44]. The homology models were aligned to their respective OPM template proteins along the Z-axis through a rigid body transformation by RMSD minimization of corresponding α-carbons (**Figure 4a**).

Using the Automatic PSF Builder extension of VMD, a Protein Structure File (PSF) was created for the two P-gp homology models. The topology file used for the PSF generation was the default CHARMM27 force field [45-47].

### 3.2. Constructing a membranous environment

A 140x140 Å palmitoyloleoylphosphatidylcholine (POPC) lipid bilayer patch composed of 546 POPC molecules was created using the Membrane Builder extension of VMD. Following manual alignment of the membrane patch to the inP-gp structure, all lipids within a cut-off distance of 1.2 Å from the protein were removed as suggested (**Figure 4b**) [48]. Water molecules generated along with the membrane and located within 3.0 Å of the protein were also removed.

While holding the protein fixed, a brief 5 ps steepest decent minimization was completed in order to relax any steric conflicts generated during construction of the system. For this and all subsequent minimizations and equilibrations, periodic boundary conditions were used with a 140x140x180 Å simulation cell. Appropriate disorder of a fluid-like bilayer was introduced through a 0.5 ns Langevin dynamics simulation performed in the NVT ensemble at 310 K (**Figure 4c**). Throughout this simulation, protein atoms were held fixed as well. The phosphate head groups of all lipids were restrained to the bilayer plane by imposing harmonic restraints on the Z components of coordinates. This capacitated mobility of the lipid molecules about the XY-plane, allowing for improved fitting of the membrane around the protein.

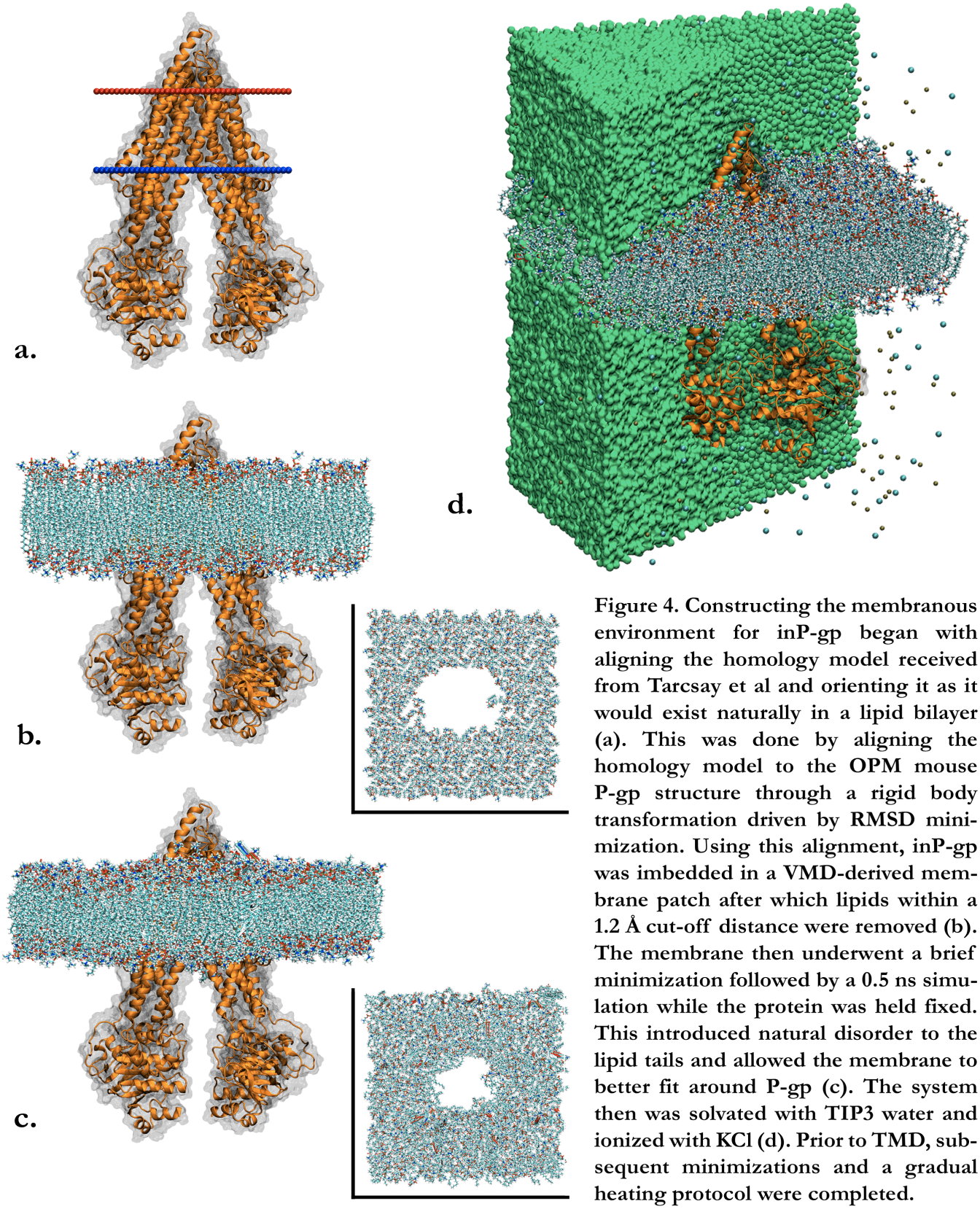


Figure 4. Constructing the membranous environment for inP-gp began with aligning the homology model received from Tarcsay et al and orienting it as it would exist naturally in a lipid bilayer (a). This was done by aligning the homology model to the OPM mouse P-gp structure through a rigid body transformation driven by RMSD minimization. Using this alignment, inP-gp was imbedded in a VMD-derived membrane patch after which lipids within a 1.2 Å cut-off distance were removed (b). The membrane then underwent a brief minimization followed by a 0.5 ns simulation while the protein was held fixed. This introduced natural disorder to the lipid tails and allowed the membrane to better fit around P-gp (c). The system then was solvated with TIP3 water and ionized with KCl (d). Prior to TMD, subsequent minimizations and a gradual heating protocol were completed.

Following an initial minimization and equilibration, the system was solvated using VMD's Solvate extension (**Figure 4d**). A solvent box composed of TIP3 water molecules was created with the same dimensions as the simulation cell (140x140x180 Å) and all water molecules within 1.5 Å of solute were removed [49]. Using Autoionize extension of VMD, $K^+$ and $Cl^-$ ions were positioned randomly throughout the solvent box to a total concentration of 200 mM. Two iterations of 5 ps steepest decent minimization were performed on the solvated and ionized system, first with the protein constrained and second with harmonic restraining forces applied to the Cα backbone. The system was then gradually heated to 310 K over 20 ps with Cα restraints.

The final inP-gp system included 354,713 atoms, 1,173 residues, 463 POPC lipids, 165 $K^+$ ions, 177 $Cl^-$ ions, and 91,283 water molecules. This was used as the starting structure in the TMD simulation. The Sav1866-based outP-gp homology model aligned using OPM data was used as the target structure.

### 3.3. Targeted molecular dynamics

VMD's targeted molecular dynamics were used to guide the I→O transition of P-gp. This was done by imposing external steering forces defined by:

$$U_{TMD} = \frac{1}{2}\frac{k}{N}[RMSD(t) - RMSD^*(t)]^2$$

where *RMSD(t)* is the instantaneous best-fit root mean square distance of the current coordinates to the target coordinates, *RMSD*(t)* is the preset RMSD (or the RMSD

between the initial and target structures) for the current timestep, $k$ is the elastic constant for TMD forces, and $N$ is the number of targeted atoms [50]. *RMSD*(t)* was initially set to 12.647 Å and decreased to 0 Å monotonically. An external spring force ($k$) of 5,865 kcal/mol/Å$^2$ was applied to the 1,173 $C_\alpha$ atoms ($N$) of P-gp as suggested in TMD simulations of similar proteins [27]. The simulation was completed in 0.5 ns at 310K and constant NVT conditions using Langevin dynamics, periodic boundary conditions, and a timestep of 1 fs/step.

# 4. RESULTS

During the TMD simulation, coordinates were saved every 500 steps, or every 500 fs, for analysis. Progression through the I→O transition can be best observed by overlaying the instantaneous structure onto the target outP-gp structure and comparing the stuctures at various time points along the trajectory (**Figure 5**). Although it is clear that the final structure of P-gp does not conform perfectly to the target structure, the steering force and duration of the simulation sufficiently reduce the overall RMSD from 12.647 Å to 7.760 Å throughout the simulation.

Perhaps the most interesting and significant observation from the simulation is that the major conformational changes in the NBDs appear to precede the shifts in the TMDs. After 200 ps, the NBDs have approached each other and begin to dimerize. Up through this point, little structural change is observed in the TMDs aside from the expected decrease in the angle between the two bundles of six helices (TMs 1-3,6,10,11 and TMs 4,5,7-9,12) that, together, constitute the two halves of P-gp. Over the next 300 ps, however, the transmembrane (TM) helices undergo significant change, resulting in the 'scissoring' motion observed from the side perspective. This sequence of events correlates well with the hypothesis that binding of ATP, stimulated by a bound substrate, causes a dimerization in the NBDs that then drives structural changes in the TMDs to create an outward facing conformation similar to that of Sav1866 [15].

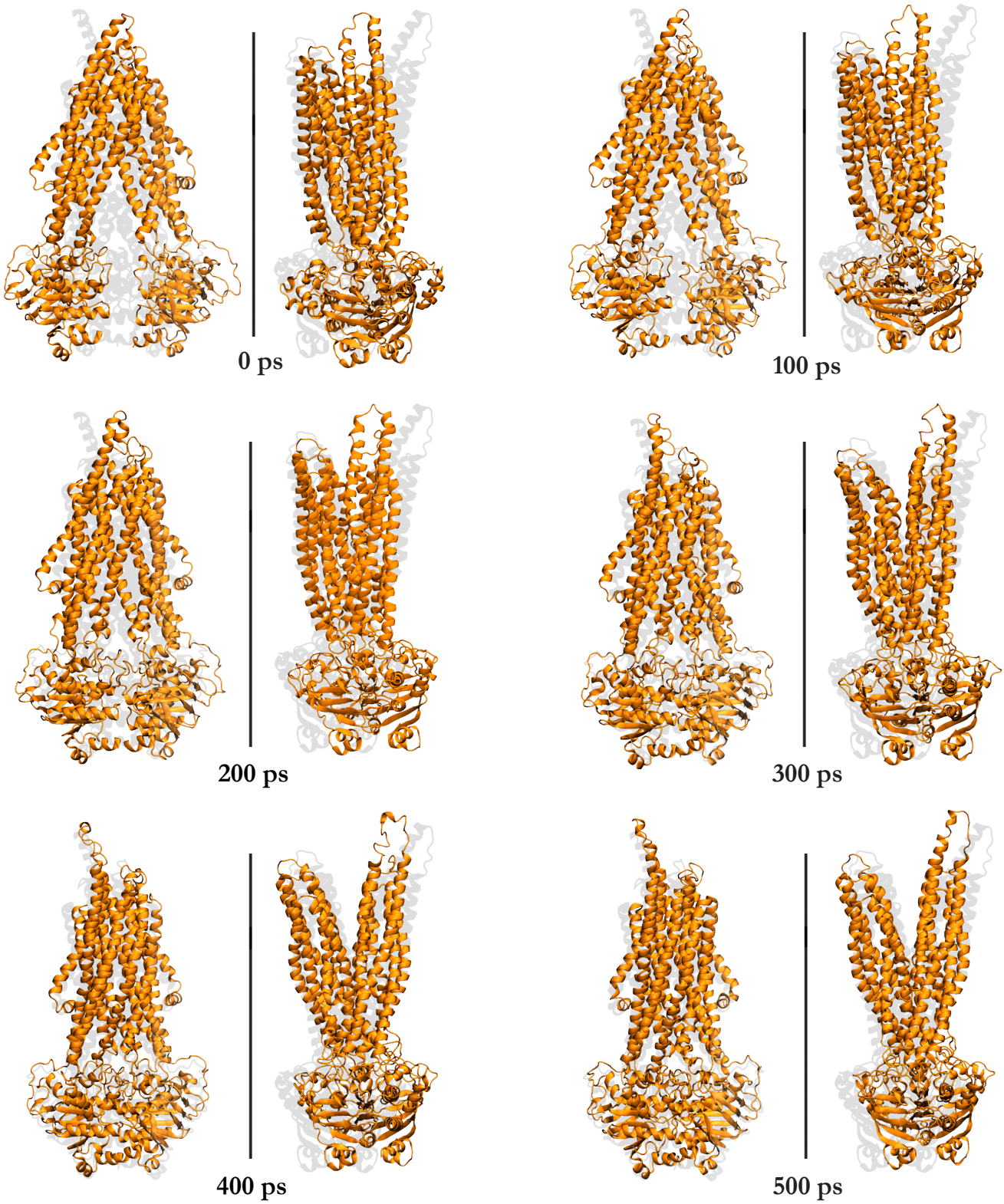


**Figure 5. Progression of the I->O transition of P-gp throughout TMD simulation. For each time step, the structure is viewed from both the front (left) and side (right). A 'ghost' of the outward-facing structure is shown for comparison at every time step.**

Although TMD simulations provide an excellent depiction of large-scale conformational changes, typical cartoon representations of the molecular structure can mask changes in the protein's pore. For this reason, the program HOLE was used to generate the radius profile of the translocation pathway of P-gp at different timesteps along the simulation (**Figure 6**) [51]. This program works by iteratively moving a point along the plane normal to the pore vector and growing it so as to find the largest sphere that can be accommodated without overlapping with the van der Walls radii of adjacent protein atoms. Once the largest sphere is determined, the point undergoes a small displacement along the direction of the pore vector a repeats the process. What results is a detailed 'casting' of a protein's pore.

At the 0 ps timestep, HOLE analysis shows P-gp to have a very large internal cavity open to both the cytoplasm and the inner lipid leaflet. The radius at the widest portion of this cavity occurs between $-70 < Z < -45$ Å, a region defined by intracellular loops (ICLs) that couple the TMDs and NBDs. The maximal radius of this region, determined by plotting the radius profile at various timesteps (**Figure 7**), is nearly 12 Å. This large cavity continues up through the lipid bilayer where drug-binding sites have been shown to reside. The volume of the cavity within the cell membrane is substantial and appears to be able to accommodate at least two compounds simultaneously as previously suggested [52]. Another characteristic of this initial inward-facing conformational state is that the pore radius nearly converges to zero at the extracellular face of the membrane domain around $Z = 30$ Å. This

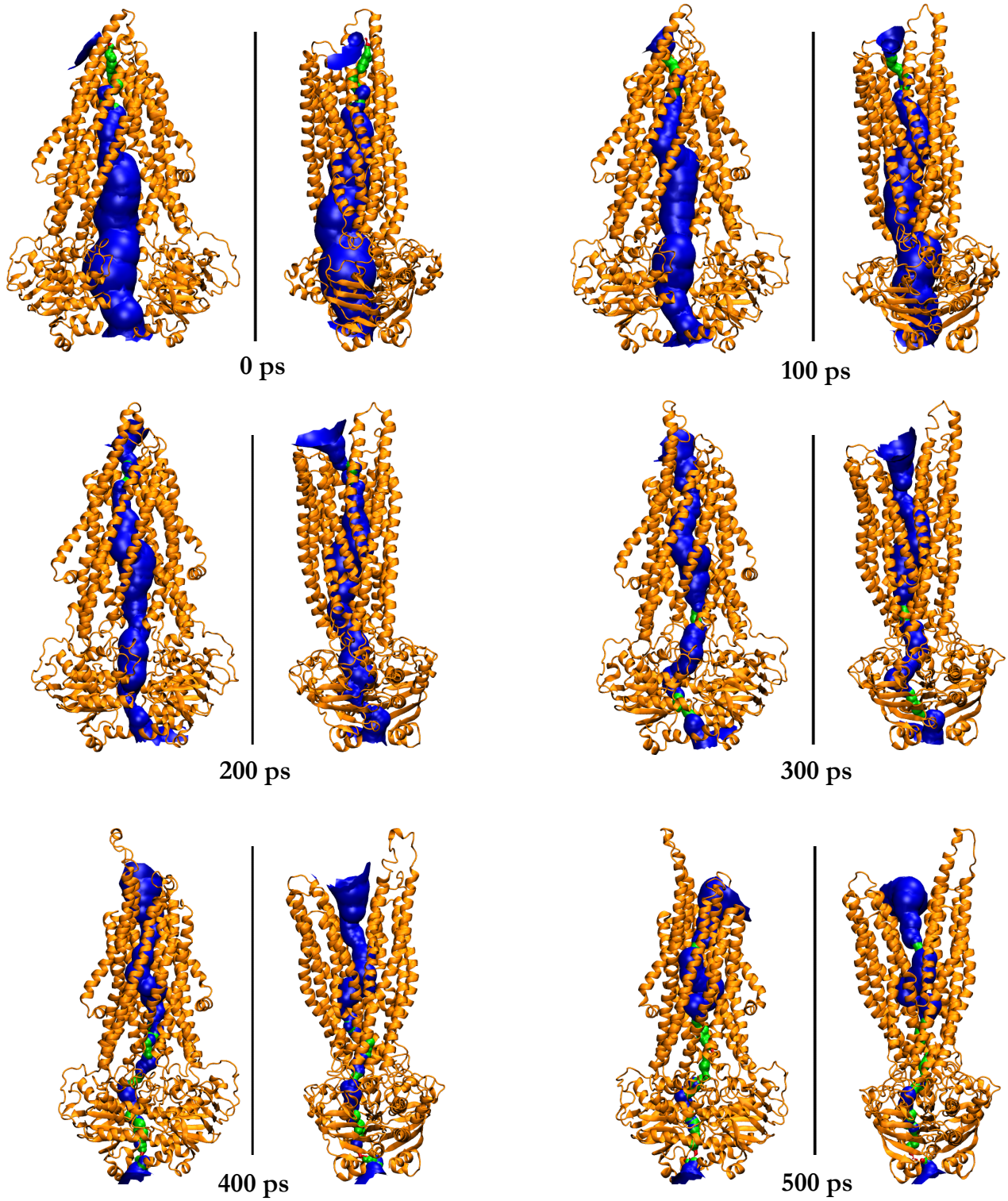


**Figure 6. Representations of the P-gp translocation pathway throughout TMD simulation as determined by HOLE. For each time step, the structure is viewed from both the front (left) and side (right). The pathway is colored such that parts inaccessible to water (pore radius < 1.15 Å) are red, water accessible parts (1.15 Å > pore radius < 2.30 Å) are green and wide areas (pore radius > 2.30 Å) are blue.**

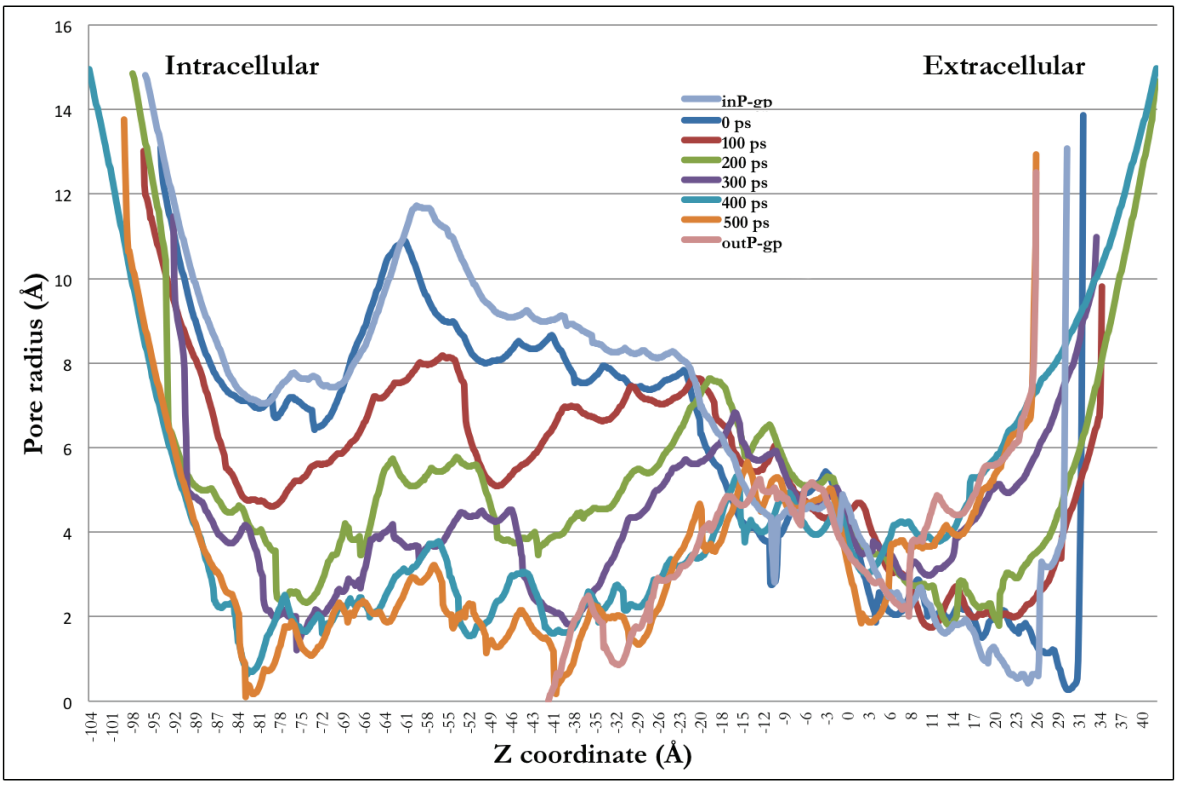


**Figure 7. Variation of the translocation pore radius throughout the I->O transition. Z-coordinates are used as they correspond to the axis to which P-gp was aligned.**

observation supports the idea that the inward-facing structure does not allow substrate access from the outer membrane leaflet nor the extracellular space [15].

Through the I→O transition of P-gp, the large cytoplasmic cavity is slowly reduced in radius as the NBDs dimerize until eventually, at 500 ps, the pore becomes occluded at this side (Z = -83 Å). Most interesting is the fact that, as the P-gp pore closes on the cytoplasmic side, it simultaneously dilates at the extracellular domain, particularly within the region Z > 5 Å. At no point, however, is a transient structure observed with both ends open. In other words, at any point along the I→O transition, P-gp is either occluded or very much constricted (radius < 2.30 Å) at one or more locations

along the translocation pathway. This observation supports the widely recognized theory that P-gp is a unidirectional efflux transporter that operates using an "alternating access" mechanism. Likening this conformational change to the motion of scissors, the joint or pivot point of P-gp appears to be the region -7 Å < Z < 4 Å where pore radius can be seen to experience little change during the simulation.

In order to better understand the conformational changes of the individual TM helices of P-gp, RMSD trajectories were calculated on α-carbons of the residues defining each TM helix (**Figure 8**). This data was provided by the OPM database entry for the mouse P-gp structure (**Figure 8a**) [44]. RMSD trajectories were then plotted for all twelve TM helices of TMD1 and TMD2 over the duration of the TMD simulation. From these plots, it is clear that not all helices undergo the same conformational changes (**Figure 8b and 8c**). The most dynamic helices in TMD1 are TM1 and TM2. For TMD2, helices TM7, TM8, and TM11 appear to undergo the most significant change. As would be expected, all of these helices are located on external surface of P-gp rather than the internal, pore-facing side. Conversely, TM6 and TM12 are pore-aligning helices and are relatively static. Due to their location, these two helices are in contact with the substrate throughout the translocation mechanism and, thus, are vital to the protein:substrate interface. TM6 and TM12 are essential to CFTR channel activity, suggesting that they are pore aligning in the CFTR structure as well. This provides evidence to our initial claim that the TMD simulation performed here on P-gp may lend information on the gating cycles of other ABC-transporters.

a.

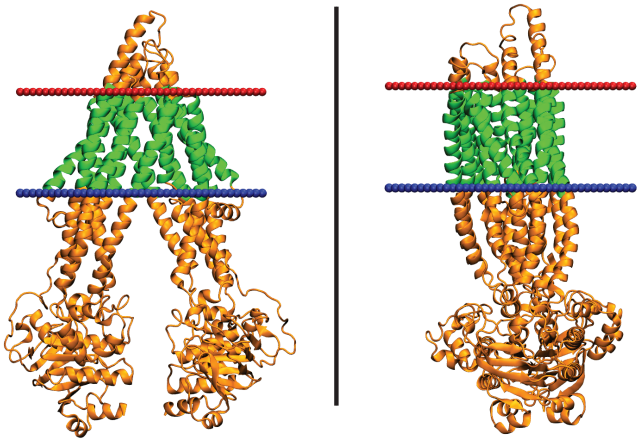

b.

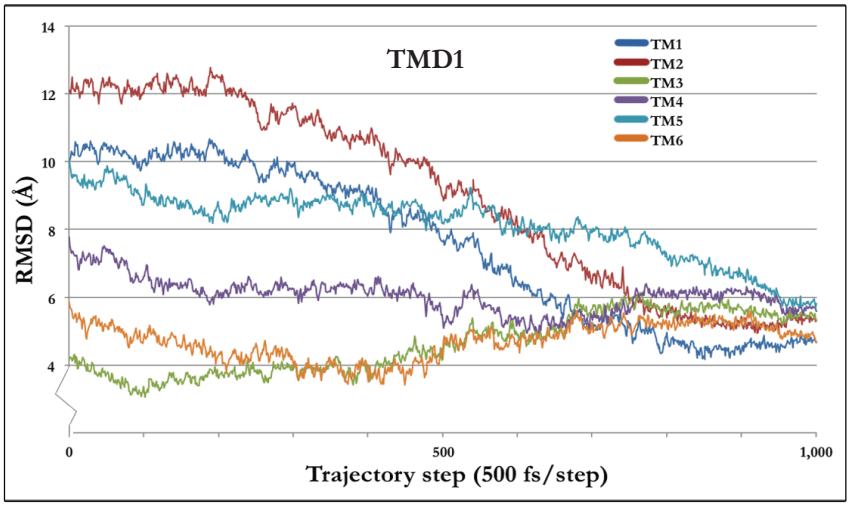


| TM Index | RMSD at 0 ps (Å) | RMSD at 500 ps (Å) | Δ RMSD (Å) |
|---|---|---|---|
| TM1 | 10.043 | 4.689 | -5.354 |
| TM2 | 12.104 | 5.334 | -6.770 |
| TM3 | 4.149 | 5.301 | 1.152 |
| TM4 | 7.776 | 5.583 | -2.193 |
| TM5 | 10.063 | 5.828 | -4.235 |
| TM6 | 5.868 | 4.665 | -1.203 |

c.

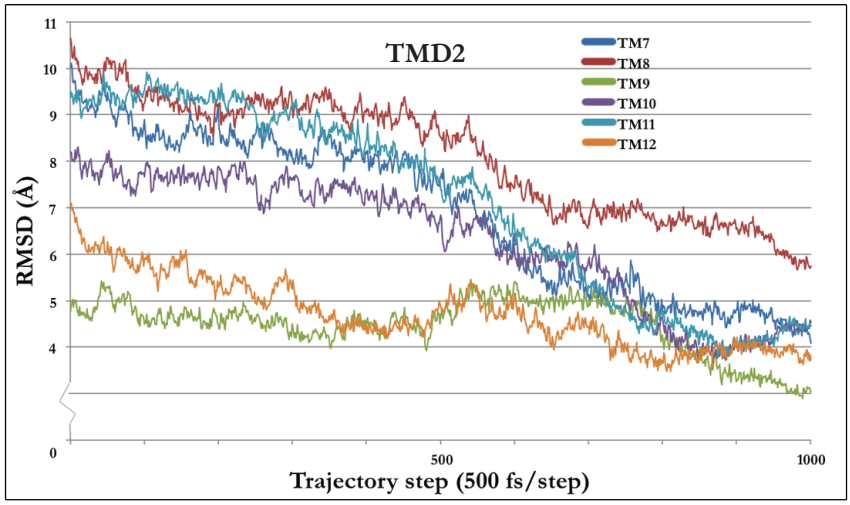


| TM Index | RMSD at 0 ps (Å) | RMSD at 500 ps (Å) | Δ RMSD (Å) |
|---|---|---|---|
| TM7 | 10.031 | 4.082 | -5.949 |
| TM8 | 10.644 | 5.744 | -4.900 |
| TM9 | 4.778 | 3.035 | -1.743 |
| TM10 | 8.189 | 4.531 | -3.658 |
| TM11 | 9.501 | 4.460 | -5.041 |
| TM12 | 7.085 | 3.715 | -3.370 |

**Figure 8. Residues defining the P-gp TMs were identified using OPM data and are depicted in green (a). RMSD values for both TMD1 (b) and TMD2 (c) were determined throughout the TMD simulation by calculating the instantaneous RMS distance between a TM's α carbons and their corresponding atoms in the target structure.**

# 5. CONCLUSION

In this study, the P-glycoprotein translocation mechanism has been simulated using targeted molecular dynamics. Results from this molecular dynamics model support several previously reported claims regarding the P-gp mechanism. The simulation demonstrates that NBD dimerization induces significant conformational changes in the TMD that result in the outward-facing state. Pore analysis agrees well with the hypothesis that P-gp is a unidirectional efflux transporter operating though an "alternating access" mechanism. This was achieved by showing that P-gp, at any point along its I→O transition, is either occluded or very much constricted at one or more locations in the translocation pathway thereby preventing bidirectional transport. In addition to providing insight into the P-gp mechanism itself, deductions can be made on the gating schemes of other ABC-transporters, such as CFTR, due to homologous structural characteristics and the conserved sequence similarity observed across members of this protein superfamily.

# REFERENCES


1. Ueda, K., et al., *THE HUMAN MULTIDRUG RESISTANCE (MDR1) GENE - CDNA CLONING AND TRANSCRIPTION INITIATION.* Journal of Biological Chemistry, 1987. **262**(2): p. 505-508.
2. Thiebaut, F., et al., *CELLULAR-LOCALIZATION OF THE MULTIDRUG-RESISTANCE GENE-PRODUCT P-GLYCOPROTEIN IN NORMAL HUMAN-TISSUES.* Proceedings of the National Academy of Sciences of the United States of America, 1987. **84**(21): p. 7735-7738.
3. Glavinas, H., et al., *The role of ABC transporters in drug resistance, metabolism and toxicity.* Current Drug Delivery, 2004. **1**(1): p. 27-42.
4. Sharom, F.J., *ABC multidrug transporters: structure, function and role in chemoresistance.* Pharmacogenomics, 2008. **9**(1): p. 105-127.
5. Zhou, S.F., *Structure, function and regulation of P-glycoprotein and its clinical relevance in drug disposition.* Xenobiotica, 2008. **38**(7-8): p. 802-832.
6. Vaz, R.J., and Thomas Klabunde, *Antitargets: Prediction and Prevention of Drug Side Effects*2008, Weinheim: Wiley-VCH.
7. Baker, M., *Making membrane proteins for structures: a trillion tiny tweaks.* Nature Methods, 2010. **7**(6): p. 429-434.
8. Blundell, T.L., et al., *Knowledge-Based Prediction of Protein Structures and the Design of Novel Molecules.* Nature, 1987. **326**(6111): p. 347-352.
9. Stenham, D.R., et al., *An atomic detail model for the human ATP binding cassette transporter P-glycoprotein derived from disulphide cross-linking and homology modeling.* Faseb Journal, 2003. **17**(13): p. 2287-+.
10. Tieleman, D.P. and M.L. O'mara, *P-glycoprotein models of the apo and ATP-bound states based on homology with Sav1866 and MalK.* Febs Letters, 2007. **581**(22): p. 4217-4222.
11. Globisch, C., I.K. Pajeva, and M. Wiese, *Identification of putative binding sites of P-glycoprotein based on its homology model.* Chemmedchem, 2008. **3**(2): p. 280-295.
12. Prevost, M., et al., *Molecular models of human P-glycoprotein in two different catalytic states.* Bmc Structural Biology, 2009. **9**.
13. Chang, G., et al., *Structure of MsbA from E. coli: A homolog of the multidrug resistance ATP binding cassette (ABC) transporters (Retraction of vol 293, pg 1793, 2001).* Science, 2006. **314**(5807): p. 1875-1875.
14. Callaghan, R., et al., *Residue G346 in transmembrane segment six is involved in inter-domain communication in P-Glycoprotein.* Biochemistry, 2007. **46**(35): p. 9899-9910.
15. Aller, S.G., et al., *Structure of P-Glycoprotein Reveals a Molecular Basis for Poly-Specific Drug Binding.* Science, 2009. **323**(5922): p. 1718-1722.
16. Pajeva, I.K., C. Globisch, and M. Wiese, *Comparison of the inward- and outward-open homology models and ligand binding of human P-glycoprotein.* Febs Journal, 2009. **276**(23): p. 7016-7026.

17. Bikadi, Z., et al., *Predicting P-Glycoprotein-Mediated Drug Transport Based On Support Vector Machine and Three-Dimensional Crystal Structure of P-glycoprotein.* Plos One, 2011. **6**(10).
18. Tarcsay, A. and G.M. Keseru, *Homology modeling and binding site assessment of the human P-glycoprotein.* Future medicinal chemistry, 2011. **3**(3): p. 297-307.
19. Chen, J., et al., *A tweezers-like motion of the ATP-binding cassette dimer in an ABC transport cycle.* Molecular Cell, 2003. **12**(3): p. 651-661.
20. Oloo, E.O., E.Y. Fung, and D.P. Tieleman, *The dynamics of the MgATP-driven closure of MalK, the energy-transducing subunit of the maltose ABC transporter.* Journal of Biological Chemistry, 2006. **281**(38): p. 28397-28407.
21. Hollenstein, K., D.C. Frei, and K.P. Locher, *Structure of an ABC transporter in complex with its binding protein.* Nature, 2007. **446**(7132): p. 213-216.
22. Pinkett, H.W., et al., *An inward-facing conformation of a putative metal-chelate-type ABC transporter.* Science, 2007. **315**(5810): p. 373-377.
23. Locher, K.P. and R.J.P. Dawson, *Structure of a bacterial multidrug ABC transporter.* Nature, 2006. **443**(7108): p. 180-185.
24. Ernst, S., et al., *Drug transport mechanism of P-glycoprotein monitored by single molecule fluorescence resonance energy transfer*, in *Multiphoton Microscopy in the Biomedical Sciences Xi*, A.K.K.S.P.T.C. Periasamy, Editor 2011.
25. Law, R.J., et al., *An ion gating mechanism of gastric H,K-ATPase based on molecular dynamics simulations.* Biophysical journal, 2008. **95**(6): p. 2739-2749.
26. Marco, E., et al., *Mechanism of activation of a G protein-coupled receptor, the human cholecystokinin-2 receptor.* Journal of Biological Chemistry, 2007. **282**(39): p. 28779-28790.
27. Weng, J., K. Fan, and W. Wang, *The Conformational Transition Pathways of ATP-Binding Cassette Transporter BtuCD Revealed by Targeted Molecular Dynamics Simulation.* Plos One, 2012. **7**(1).
28. Feynman, R.P.L., R.B. & Sands, M, *The Feynman Lectures in Physics Vol. I*1963, Reading: Addison-Wesley. 3-6.
29. Schlitter, J. and M. Klahn, *The free energy of a reaction coordinate at multiple constraints: a concise formulation.* Molecular Physics, 2003. **101**(23-24): p. 3439-3443.
30. Schlitter, J., et al., *TARGETED MOLECULAR-DYNAMICS SIMULATION OF CONFORMATIONAL CHANGE - APPLICATION TO THE T -- R TRANSITION IN INSULIN.* Molecular Simulation, 1993. **10**(2-6): p. 291-&.
31. Weng, J.-W., K.-N. Fan, and W.-N. Wang, *The Conformational Transition Pathway of ATP Binding Cassette Transporter MsbA Revealed by Atomistic Simulations.* Journal of Biological Chemistry, 2010. **285**(5).
32. Swift, R.V. and J.A. McCammon, *Catalytically requisite conformational dynamics in the mRNA-Capping enzyme probed by targeted molecular dynamics.* Biochemistry, 2008. **47**(13): p. 4102-4111.

33. Huang, H., E. Ozkirimli, and C.B. Post, *Comparison of Three Perturbation Molecular Dynamics Methods for Modeling Conformational Transitions.* Journal of Chemical Theory and Computation, 2009. **5**(5): p. 1304-1314.
34. Riordan, J.R., et al., *Identification of the Cystic-Fibrosis Gene - Cloning and Characterization of Complementary-DNA.* Science, 1989. **245**(4922): p. 1066-1072.
35. Sorscher, E.J., S.M. Rowe, and S. Miller, *Mechanisms of disease: Cystic fibrosis.* New England Journal of Medicine, 2005. **352**(19): p. 1992-2001.
36. O'Sullivan, B.P. and S.D. Freedman, *Cystic fibrosis.* Lancet, 2009. **373**(9678): p. 1891-1904.
37. Amaral, M.D., et al., *Solubilizing mutations used to crystallize one CFTR domain attenuate the trafficking and channel defects caused by the major cystic fibrosis mutation.* Chemistry & biology, 2008. **15**(1): p. 62-69.
38. Dokholyan, N.V., et al., *Phenylalanine-508 mediates a cytoplasmic-membrane domain contact in the CFTR 3D structure crucial to assembly and channel function.* Proceedings of the National Academy of Sciences of the United States of America, 2008. **105**(9): p. 3256-3261.
39. Callebaut, I., J.P. Mornon, and P. Lehn, *Atomic model of human cystic fibrosis transmembrane conductance regulator: Membrane-spanning domains and coupling interfaces.* Cellular and Molecular Life Sciences, 2008. **65**(16): p. 2594-2612.
40. Mornon, J.P., P. Lehn, and I. Callebaut, *Molecular models of the open and closed states of the whole human CFTR protein.* Cellular and Molecular Life Sciences, 2009. **66**(21): p. 3469-3486.
41. Dawson, D.C., et al., *Cystic Fibrosis Transmembrane Conductance Regulator: Using Differential Reactivity toward Channel-Permeant and Channel-Impermeant Thiol-Reactive Probes To Test a Molecular Model for the Pore.* Biochemistry, 2009. **48**(42): p. 10078-10088.
42. Humphrey, W., A. Dalke, and K. Schulten, *VMD: Visual molecular dynamics.* Journal of Molecular Graphics, 1996. **14**(1): p. 33-&.
43. Schulten, K., et al., *Scalable molecular dynamics with NAMD.* Journal of Computational Chemistry, 2005. **26**(16): p. 1781-1802.
44. Lomize, A.L., et al., *OPM: Orientations of proteins in membranes database.* Bioinformatics, 2006. **22**(5): p. 623-625.
45. Feller, S.E., et al., *Molecular dynamics simulation of unsaturated lipid bilayers at low hydration: parameterization and comparison with diffraction studies.* Biophysical journal, 1997. **73**(5): p. 2269-79.
46. MacKerell, A.D., et al., *All-atom empirical potential for molecular modeling and dynamics studies of proteins.* Journal of Physical Chemistry B, 1998. **102**(18): p. 3586-3616.
47. Mackerell, A.D., M. Feig, and C.L. Brooks, *Extending the treatment of backbone energetics in protein force fields: Limitations of gas-phase quantum mechanics in reproducing protein conformational distributions in molecular dynamics simulations.* Journal of Computational Chemistry, 2004. **25**(11): p. 1400-1415.
48. Kandt, C., W.L. Ash, and D.P. Tieleman, *Setting up and running molecular dynamics simulations of membrane proteins.* Methods, 2007. **41**(4): p. 475-488.

49. Jorgensen, W.L., et al., *COMPARISON OF SIMPLE POTENTIAL FUNCTIONS FOR SIMULATING LIQUID WATER*. Journal of Chemical Physics, 1983. **79**(2): p. 926-935.
50. Hummer, G. and I.G. Kevrekidis, *Coarse molecular dynamics of a peptide fragment: Free energy, kinetics, and long-time dynamics computations*. Journal of Chemical Physics, 2003. **118**(23): p. 10762-10773.
51. Smart, O.S., et al., *HOLE: A program for the analysis of the pore dimensions of ion channel structural models*. Journal of Molecular Graphics & Modelling, 1996. **14**(6): p. 354-&.
52. Loo, T.W., M.C. Bartlett, and D.M. Clarke, *Simultaneous binding of two different drugs in the binding pocket of the human multidrug resistance P-glycoprotein*. Journal of Biological Chemistry, 2003. **278**(41): p. 39706-39710.